1. Problem

Overview:

Capsular contracture (CC) is the most common complication of breast reconstruction and augmentation surgery (Dancey et al.). CC is defined as "a tight or constricting scar tissue capsule forming around a [breast] implant, often distorting the breast shape and resulting in chronic pain" (Guimier et al.). CC is qualitatively evaluated into four tiers of severity based on the Baker Classification System (Spear and Baker):

Class I: Breast absolutely natural; no one could tell breast was augmented

Class II: Minimal contracture; surgeon can tell surgery was performed, but patient has no complaint

Class III: Moderate contracture; patient feels some firmness

Class IV: Severe contracture; obvious just from observation

Pathogenesis:

Foreign bodies implanted in the body can elicit an immune response that fibrously encapsulates the implanted object(s) (Safran et al.). In the case of CC, immunological factors and bacterial contamination have been proposed as potential causes. However, the widely accepted school of thought suggests that CC is a result of macrophage response to the trauma of breast implant surgery (Bachour et al.). Transitioned and activated macrophages derived from monocytes produce anti-inflammatory cytokines (including TGF-β), that promote epithelial-to-mesenchymal transition (EMT). EMT results in the phenotypic transformation of epithelial cells to myofibroblasts that produce α-smooth muscle actin (α-SMA) and collagen fibers (forming a net around the implant). The presence of α-SMA allows the myofibroblasts to contract, pulling on the collagen fiber network, tightening the capsule around the implant, and producing the pain associated with capsular contracture (Braga et al.; Abu El-Asrar et al.; Younesi et al.). (See Appendix A for more detail)

Treatment:

Non-surgical treatments for CC include physical massages to break up the capsule or injection of leukotriene/COX-2 inhibitors to suppress inflammation. However, these methods are considered an ineffective long term solution as the underlying causes of the capsule remain untreated (Hidalgo and Sinno). Grade III and IV cases often lead to patients undergoing a capsulectomy, the partial or total surgical removal of the capsule.

Incidence Rates:

Incidence rates of CC vary from 3-20% (Lee et al.), depending on numerous risk factors. Among them, rates are particularly high for two cases of immediate breast reconstruction (IBR): implant replacement after a capsulectomy, and direct-to-implant breast reconstruction after mastectomy. CC recurrence rates in capsulectomy patients are as high as 53% (Hester et al.). Breast cancer patients who undergo mastectomy and IBR are also at higher risk due to post-mastectomy radiotherapy (PMRT), which can drive incidence rates as

high as 48% (Vinsensia et al.).

Patient Population:

CC threatens a massive and increasing patient population. In 2022, nearly 1.9 million breast augmentations were performed globally. In the US, more than 240,000 breast augmentations were performed in 2022 (International Society of Aesthetic Plastic Surgery), while over 157,000 breast reconstructions were performed in 2023 (American Society of Plastic Surgeons). The number of breast reconstructions has consistently increased the past few years, with the rate of implant-based reconstruction outpacing autologous reconstruction. In 2017, 29% of mastectomies lead to IBR, where 18% of those IBRs are followed by PMRT (Razdan et al.). Given roughly 30,000 mastectomies in the US annually (Roskam et al.), the high incidence rate for PMRT alone directly threatens 1,500 patients, let alone capsulectomy patients and the general threat to the entire breast reconstruction population. The lack of effective, long term treatment in this population demands a breast implant-related solution that reduces the incidence of CC.

2. Design Overview

Objective:

An implantable product that releases an EMT-targeting therapeutic to prevent capsule development and contraction, for application during an IBR.

Product:

The product is a sheet of acellular dermal matrix (ADM) augmented with a drug loaded hydrogel. The drug is pirfenidone, the hydrogel is poly(ethylene glycol), or PEG, and the ADM is Allergen's AlloDerm Select product. The drug is conjugated to PEG solution, which is then cross-linked as a hydrogel throughout the ADM sheet. This combination sheet is designed to be cut and stitched together by a surgeon to fully wrap any existing breast implant prior to implantation during an IBR.

Motivation for Design:

Several candidate EMT-targeting drugs were considered, including fibroblast and TGF-β activation inhibitors like nintedanib and losartan (FDA approved for fibrosis in other organs), leukotriene receptor antagonists like montelukast and zafirlukast (used off-label for CC), a monoclonal antibody called fresolimumab (investigated for fibrosis in other organs), and corticosteroids like triamcinolone and prednisone (used off-label for CC). While many show potential to reduce capsule thickness and fibroblast count in animal models, pirfenidone is the strongest option because it directly address EMT by downregulating TGF-β, is already FDA-approved for addressing fibrosis, shows promise for antifibrotic application in several organs, and has been shown to reverse CC in humans (Veras-Castillo et al.; Gancedo et al.).

Pirfenidone poses two challenges. First, its oral administration relies on systemic delivery. First-pass

metabolism and off-target absorption, especially in the gastro-intestinal (GI) tract, lead to unintended consequences with only a fraction of the drug reaching its target location. Second, pirfenidone has a short half-life of roughly 3 hours, necessitating thrice daily administration and increasingly severe side effects with higher doses. Though pirfenidone's symptoms are generally very mild, it can cause GI issues like nausea, skin-related issues like photosensitivity, and liver issues (Costabel et al.), each of which are attributable to and can be aggravated by drug concentration spikes via oral administration. To mitigate maximum plasma concentration and associated symptoms, pirfenidone is labeled to be taken with food, but food only further reduces drug absorption by 16% (Drugs@FDA).

These challenges encourage local, continuous delivery, which can mitigate side effects by eliminating spikes and gaps in drug delivery and drastically reducing systemic distribution of high doses. Hydrogels are a common drug vehicle, for example in breast cancer treatments, because they provide a biocompatible platform for tuning release characteristics (Lin et al.). Synthetic hydrogels were favored over natural ones for longer shelf-stability. PEG was selected for its highly engineerable degradation rates and drug release methods (Vigata et al.) and for its slight favorability over PLGA in in vivo testing of fibrotic development around implanted hydrogels (Kim et al.).

A thin hydrogel layer alone, though highly cross-linked, may not hold stably around a breast implant and could lead to irregular degradation and drug distribution into breast tissue. To provide a structurally sound housing for the hydrogel, we chose to impregnate ADM sheets with the drug-loaded hydrogel. Clinical application of ADMs as structural support in IBRs is established and increasing year-over-year, so this combination of familiar components offers new utility with a low barrier to clinical acceptance. While ADM is generally used as a sling to help support the lower pole, current clinical application includes fully wrapping implants with ADM (Nahabedian), and the practice has shown potential to reduce the rate of CC (Bassetto et al., Cheng et al.).

In a study comparing bovine, porcine, and human derived ADM, bovine had the highest CC rate (Pires et al.). Therefore, we favored a human-derived product over bovine-derived dermal regeneration templates and other bovine- or porcine-derived ADMs. In particular, we chose Allergen's Alloderm product because the FDA evaluated a lower risk for AlloDerm than similar, human-derived ADM competitors (FDA, Safety Communication).

3. Description of Design Components

Pirfenidone

Pirfenidone is a FDA-approved drug for idiopathic pulmonary fibrosis (IPF). Its antifibrotic properties were investigated as early as 1990 and continue to be investigated for fibrosis in the liver, kidney, heart, and

breasts, among other conditions (Cho and Kopp). Officially called 5-methyl-1-phenyl-1H-pyridin-2-one, pirfenidone has the molecular formula $C_{12}H_{11}NO$ with molar mass of 185.22g/mol or 0.185kDa. It is an axially chiral molecule composed of a phenyl and pyridinone ring. It can be synthesized with >99.5% purity.

Pirfenidone's mechanism of action has not been established (Drugs@FDA). Applications of pirfenidone in fibrotic conditions like Dupuytren's disease and IPF commonly recognize downregulation of fibrogenic mediators, including growth factors like TGF-β, platelet-derived growth factor (PDGF), and basic fibroblast growth factor (bFGF), as well as cytokines like tumor necrosis factor alpha (TNF-α) and interleukin-1 beta (IL-1β) (Schaefer et al.; Zhou et al.).

Pirfenidone is commonly administered as oral tablets or capsules thrice daily. Tablet dosage increases from 267 mg in week 1 to 534 mg in week 2, then 801 mg thereafter. Pirfenidone's effects are indifferent to obesity, race, and gender (Drugs@FDA).

Pirfenidone's pharmacokinetics are characterized by its oral administration. After absorption in the intestines, pirfenidone passes into blood after first-pass metabolism in the liver. Pirfenidone is systemically distributed by binding to human plasma proteins, reaching maximum concentration after 0.5-4 hours. Food significantly decreases the rate and extent of absorption, reducing max plasma concentration by 49% for an 800mg dose. Absolute bioavailability is 46% in rats (Togami et al.), but undetermined in humans (Drugs@FDA). Mean half-life is around 3 hours, with roughly 80% of the drug excreted in urine as the metabolite 5-carboxylic acid. There is "no significant accumulation of the drug after repeated dosing" (Cho and Kopp, Shi et al.) and pharmacokinetics are not age-dependent (Babovic-Vuksanovic et al.).

PEG

PEG is a hydrophilic, flexible polymer commonly used as a drug carrier due to its low immunogenicity and toxicity. PEG's structure consists of repeating units of ethylene oxide and is characterized by its molecular weight (MW), which depends on the length of the polymer (ex. PEG6000 has a MW of 6000 g/mol).

PEG has been extensively applied clinically for drug delivery. PEGylation, or the method of covalently conjugating drugs to PEG, has produced 38 FDA-approved therapeutics, none of which address fibrosis. PEGylation improves the pharmacokinetics of small molecules, proteins, liposomes, and antibody fragments, for example by shielding proteins from immune system recognition, increasing hydrodynamic size, or altering receptor binding. As a hydrogel, PEG has been FDA-approved as burn and wound dressings and as laxatives. Drug-carrying PEG hydrogels include injectables for ototoxicity (Chen et al.) and cancer (Zang et al.) and even a sprayable formulation loaded with pirfenidone for treating IPF (Bao et al.).

The primary in vivo mechanism of degradation for PEG is hydrolysis, after which it is believed that cells pinocytose the degraded PEG and deliver to the bloodstream (Baumann et al.). Though dependent on size, it is

often largely unmetabolized, with up to 96% of PEG6000 cleared by urine 12 hours after it enters the blood (Webster et al.).

ADM

ADMs are tissue scaffolds derived from humans, cows, or pigs. Donor tissue is decellularized by lysing with chemical detergents, dehydrated by freeze-drying or vacuum-pressing, and optionally sterilized with ethylene oxide or irradiation (Macadam and Lennox). ADM's structure consists of collagen fibers in the same extracellular matrix (ECM) structure as regular dermal tissue. Human-derived ADM can be produced with 75-93% porosity (Tao et al.). Porosity index under 120mmHg pressure is 0.03mL/cm^2/min for AlloDerm (Carruthers et al.). Alloderm ADM thicknesses range from 1.6 to 3.2mm.

Clinically, ADM is used in breast reconstruction to provide support to the lower pole and is a major factor in increasing rates of immediate breast reconstruction. The tissue matrix is recolonized by host cells and becomes vascularized (Bohac et al.). ADM reduces contracture by allowing collagen to grow perpendicularly to the implant surface, rather than aligning parallel to the implant surface. This disorganization disperses the contractile forces applied by myofibroblasts and mitigates their effect.

ADM is both biocompatible and degradable. It undergoes constructive remodeling rather than pure degradation, promoting integration with the host tissue and mitigating the foreign body response. After implantation, the matrix is infiltrated by host cells and remodeled as endothelial and stromal cells vascularize the matrix. This process typically begins within weeks and continues over several months with AlloDerm showing partial degradation by 112 days and volume stabilization by six months post-implantation (Smart et al.; Sclafani, A P et al.).

4. Drug Load, Dose, and Therapeutic Window

The total drug load requirement for the product depends on pirfenidone's release profile and modifications to its standard dosage for local delivery in this off-label application.

Pirfenidone's release rate is dominated by how quickly its bonds to the PEG hydrolyze. Due to its size, pirfenidone's diffusion rate does not significantly delay release, nor should the release profile change with the hydrogel's pore size as the product degrades. (See Appendix B for details) Given ester bonds to PEG, pirfenidone will release at an exponentially decaying rate over several weeks, as demonstrated with ester-bonded drugs in solution and in human plasma. For both studies, roughly 10% of the drug load is released on the first day, limiting the total drug load to 10 times the daily dose for local delivery. While the product's current design solely relies on ester-bonding drugs with a single linker type, the drug's release rate could be tuned in a later design iteration by using β-eliminative linkers with varying cleavage rates.

Pirfenidone's daily dose for local delivery can be loosely rationalized from oral administration in animal

and human models. In an animal model, 46% of orally administered pirfenidone reached the blood, and 52% of pirfenidone in the bloodstream reached the lungs. As such, the amount of orally administered pirfenidone available to local tissue can be approximated as roughly 25% of the oral dose. In human trials for reversing CC with pirfenidone, 600mg was orally administered thrice daily for 6 months for a total daily dose of 1.8g (Togami et al.). Together, these findings suggest a locally delivered daily dose of 1.8g/4 = 450mg for treating CC. Given 10% release on the first day, the maximum drug load for the hydrogel should not exceed 4500mg.

Predicting the product's therapeutic window first requires estimating the minimum therapeutically effective dose of pirfenidone for treating CC. For IPF, 50% of pirfenidone's max therapeutic effect using 800mg thrice daily was achieved by a plasma concentration of 1.73mg/L (Wang et al.), where the mean plasma concentration for the maximum daily dosing can be estimated as 8.73mg/L. The linear relationship between dose and plasma concentration suggests that roughly 1.73/8.83 = 19.6% of the daily oral dose is sufficient for 50% therapeutic effect for IPF. Applying this assumption to CC is tenuous, because the comparison is between different conditions and orally-administered pirfenidone likely accumulates in breast tissue differently than the lungs. Nonetheless, given the approximation of 450mg as the locally delivered maximum daily dose, 450*19.6% = 88mg gives a starting assumption for the minimum effective daily dose for addressing CC.

Given this assumption that 19.6% of the daily dose is the minimum for 50% effectiveness, the therapeutic window of this application is approximately 42 days, based on the release profile of small-molecule drugs from PEG hydrogels in solution. Animal models exploring sustained release of antifibrotic drugs from implant wrappings have shown that this time-scale is sufficient to demonstrate significant disruption to collagen organization and reduction in TGF-β, fibroblast count, and capsule thickness (Huh et al.; Acuner et al.).

5. PEG Hydrogel Design

The PEG macromers must be less than 30 kDa because larger chains are filtered out in the kidneys and can distribute and accumulate within various tissues throughout the body (Baumann et al.). This limit encourages mass-efficient methods of conjugating pirfenidone.

The PEG structure must be able to crosslink with itself and bond to pirfenidone. Therefore, it must have more than 2 ends or arms, with at least half devoted to cross-linking to form a stable hydrogel. Most manufacturers only produce 4-arm and 8-arm PEG usually, where higher arm count is preferable to efficiently support higher drug loads. 8-arm PEG (5 kDa) with 4 amine groups and 4 acrylate groups is an ideal option, as offered by Creative PEGWorks. The acrylate arms can covalently cross-link with thermal activation to create the hydrogel network, while the amine arms can bond to pirfenidone through a linker molecule.

Dendrimers are an ideal linker structure because they can expand the drug loading capacity by offering multiple conjugations per PEG arm. Dendrimers are a class of synthetic polymer molecules with radially

symmetric tree-like arms stemming from a core. Arm count depends on rounds or generations of synthesis, where generation 0 is the core, generation 1 adds 2 arms, and each following generation squares the count. These arms can be terminated with functional groups and used to link small molecules to polymer scaffolds (Abbasi et al.).

8-arm 2,2-bis(hydroxymethyl)propionic acid, or Bis-MPA dendrimers satisfy requirements for this application. Firstly, they are degradable and non-toxic (Namata et al.). Secondly, Bis-MPA dendrimers have a trimethylolpropane, or TMP core with a carboxyl group for amide bonding with PEG, while the dendrimer's hydroxyl-terminated arms can form hydrolyzable ester bonds with pirfenidone. MW is roughly 5kDa for commercially available 8-arm Bis-MPA dendrimers, creating with the 5kDa PEG molecule a 25kDa total mass that satisfies the 30kDa size limit. The hydrogel structure is simplified and illustrated in Figure 22.

The equation below models the amount of pirfenidone that can be loaded as a function of the volume and porosity of the ADM, the density and % concentration of PEG in the hydrogel precursor solution, the number of pirfenidone molecules per PEG molecule, and the molecular weights of pirfenidone and the PEG.

$$m_{pirfenidone} = V_{ADM} \cdot P_{ADM} \cdot \rho_{PEG\ solution} \cdot \frac{C_{PEG\ solution}}{100} \cdot \frac{N_{pirfenidone}}{MW_{PEG}} \cdot MW_{pirfenidone}$$

Equation 1: Drug loading capacity based on design details

Assuming 50% PEG solution, a 2.4mm thick ADM, and 85% ADM porosity, the drug loading capacity ranges from 3-10g for various breast implant sizes. The main driver of loading capacity is the number of pirfenidone molecules that can be conjugated to each PEG macromer. While the proposed design relies entirely on off-the-shelf products and is limited by the PEG's arm count, custom ordered or synthesized PEG with more arms and minimized molecular weight could significantly improve the loading capacity of the product.

A high concentration solution is also critical to increase the drug load capacity. Generally, hydrogels are derived from solutions with PEG concentration at 20% or below because higher concentrations prohibitively increase viscosity for injection applications. In this application, a stiffer hydrogel based on a 50% solution is acceptable because the hydrogel serves primarily as a structural platform from which to release a drug. 8-arm, 12.5kDa, step-growth-polymerized 20% PEG hydrogels exhibit stiffness ~50kPa, and a larger, 25kDa PEG platform should trend to lower stiffnesses (Lee et al.). These stiffnesses are comparable to dermal tissue, which has been reported at 40kPa (though values range widely depending on the test) (Feng et al.; A et al.). Nonetheless, strictly increasing concentration will impact stiffness, and viability studies are required to demonstrate that this high concentration can be manufactured and implanted without adverse effects.

PEG degradation over the product's lifetime does not threaten patient safety. PEG degrades hydrolytically and consistently over time with degradation rates varying: one clinical study shows 40% degradation of PEG over 12 weeks in an animal model, whereas other PEG hydrogels, such as DuraSeal®, can

take 4-8 weeks to be completely absorbed in vivo with no adverse tissue responses (Browning et al., Kim et al., US FDA,). PEG's degradation can be tuned by modifying monomer molecular mass, crosslinkers, or incorporating self-cleaving linkers, and this controlled degradation behavior combined with PEG's established biocompatibility, low toxicity, and rapid renal clearance for low molecular weight chains makes it highly suitable for biomedical coatings (Ashley et al.).

6. Product Manufacturing

To enable conjugation to the Bis-MPA dendrimers, a solution of pirfenidone will be succinylated using succinic anhydride to add a carboxyl group to the structure (creating pirfenidone–COOH). This process functionalizes the drug (allowing it to form ester bonds with the dendrimers) while maintaining the overall structure of the molecule and its safety for use inside the body (Birajdar et al.). To conjugate dendrimers to PEG, the carboxylic cores of the dendrimers will be activated with carbonyl diimidazole for amidation with the amine-functionalized PEG arms (Stenstrom et al.).

From there, the dendrimer-PEG system will be added to the aqueous succinylated pirfenidone to create a drug-loaded solution with PEG concentration from 20% to 50% (w/v), which is soaked into dehydrated ADM. Vacuum pressure can be applied to encourage permeation of the viscous solution into the dehydrated ADM (Negishi et al.). Common high energy methods like UV can destabilize pirfenidone, so the solution will be crosslinked via heat-assisted thiol-Michael addition, producing step-growth polymerization (Capanema et al.; Vanitha et al.; Gao et al.).

7. Product Application

The device will be supplied in a dehydrated state to maximize shelf life and simplify logistics. Prior to use, the PEG/ADM composite should be rehydrated in sterile saline or a drug-compatible buffer. Based on experimental guidance from ADM manufacturers and PEG hydrogel protocols, we recommend rehydration for at least 2 hours prior to implantation. This duration ensures adequate saturation of both PEG and ADM components, restoring flexibility and optimal handling (AlloDerm IFU; Browning et al.; Luong et al.).

After hydration, the pre-shaped ADM/PEG sheet will fit the dimensions of the selected implant, allowing for easy circumferential wrapping around the silicone gel implant. The edges of the ADM would be brought together and sutured with absorbable suture—such as 2-0 or 3-0 polydioxanone (PDS)—to form a full 360° encapsulation of the implant (Bojanic et al.; Parcells et al.).

In preparing for surgery, the operating surgeon should account for the added volume and surface area of the ADM/PEG wrap when selecting the implant size. Following mastectomy, the prepared ADM/PEG wrapped implant can be inserted using either a submuscular or prepectoral technique, depending on the patient's

anatomical and oncological needs. For submuscular placement, the ADM/PEG composite can be sutured to the muscle and inframammary fold, and for prepectoral placement, the wrapped implant can be anchored directly to the chest wall to prevent movement post implantation. Drains can be placed and the incision can be closed following standard immediate implant-based breast reconstruction protocols (Bojanic et al.; Parcells et al.).

Figures

Figure 1:Grade IV CC in right breast (Patel et al.)

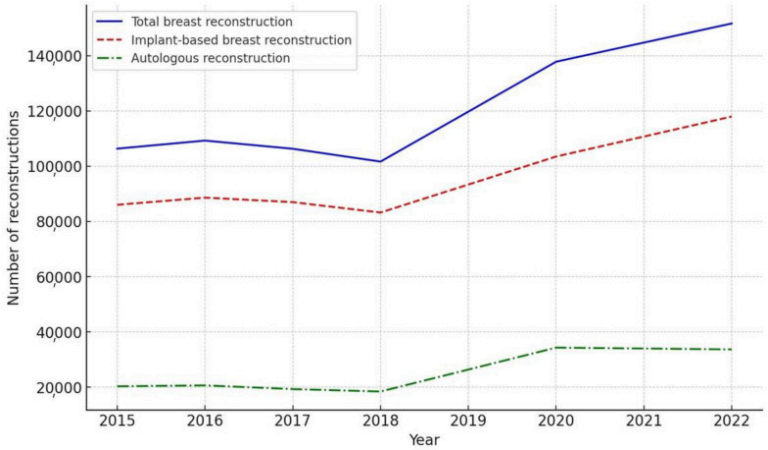

Figure 2: Trend of breast reconstructions in the US (Eun Hong and Kang)

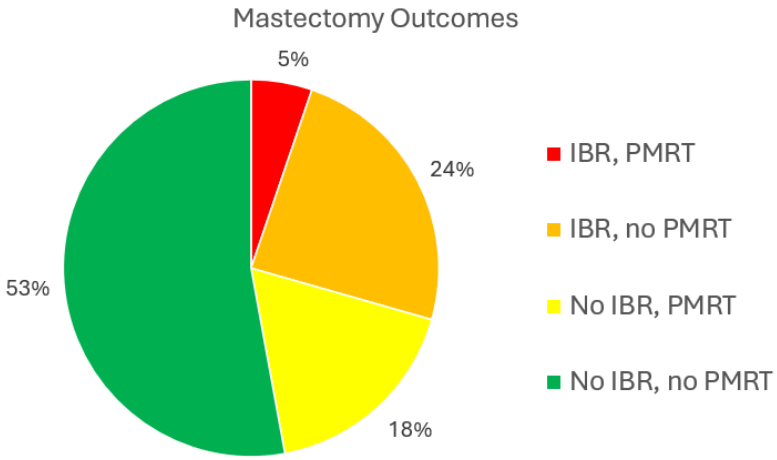

Figure 3: Mastectomy outcomes

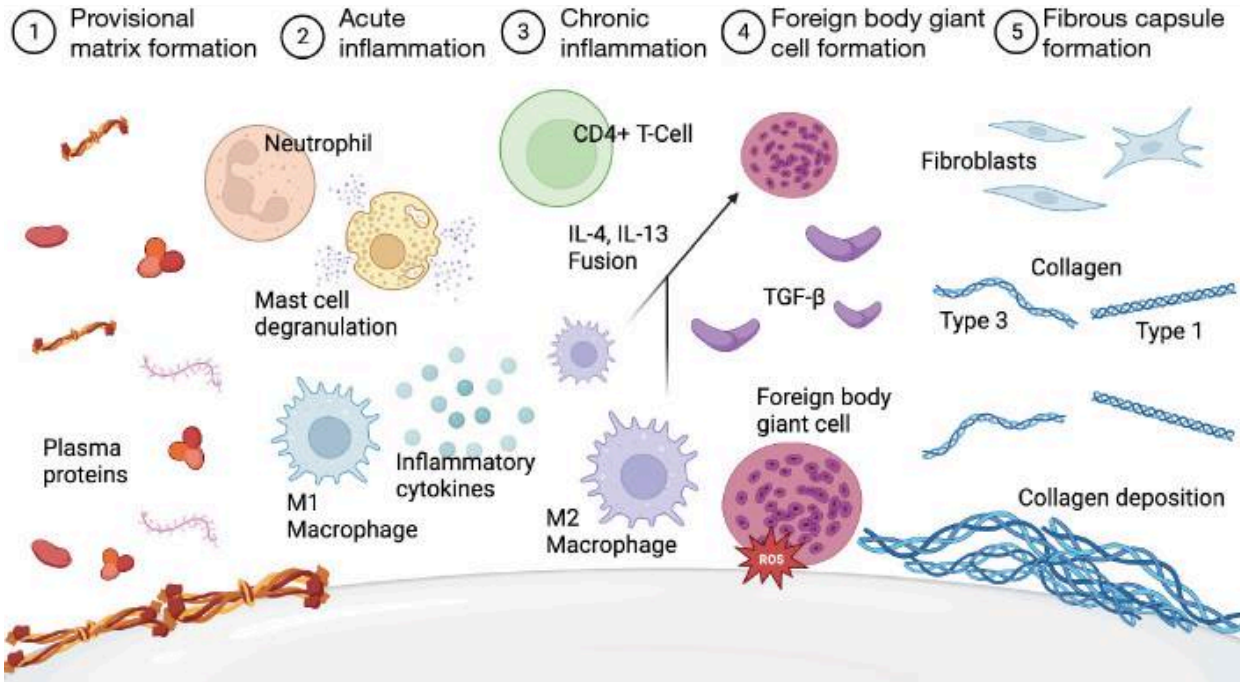

Figure 4: Cell development and products through various steps of the healing process (Gorgy et al.)

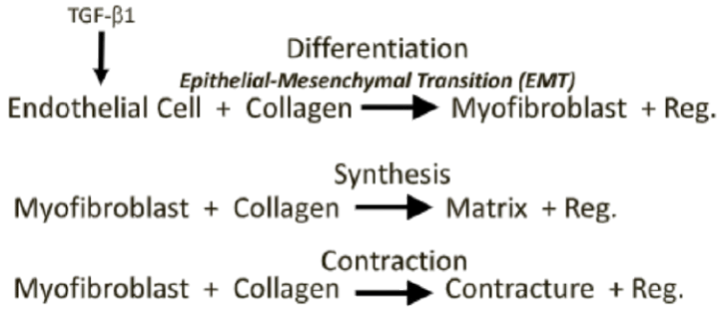

Figure 5: Unit cell processes of EMT as they relate to capsular contracture

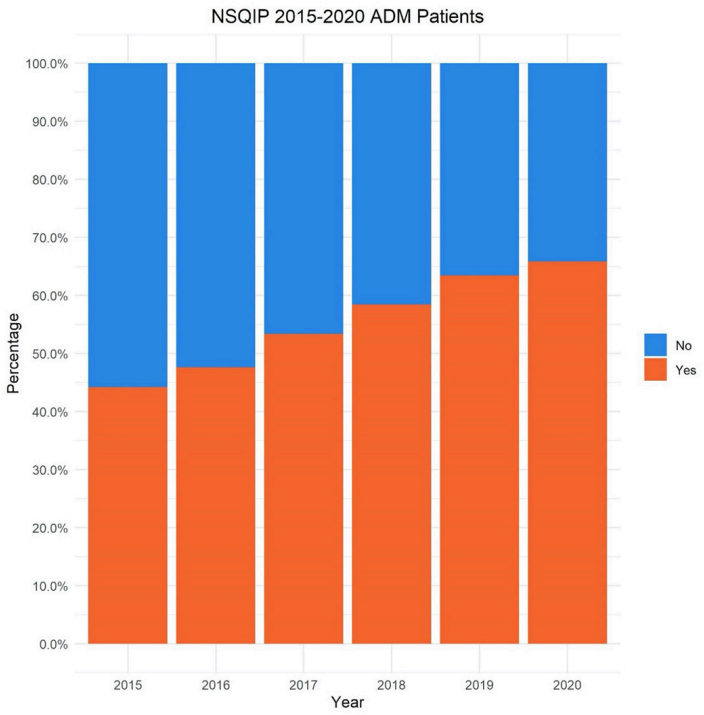

Figure 6:ADM use in immediate, direct-to-implant breast reconstruction (Graziano et al.)

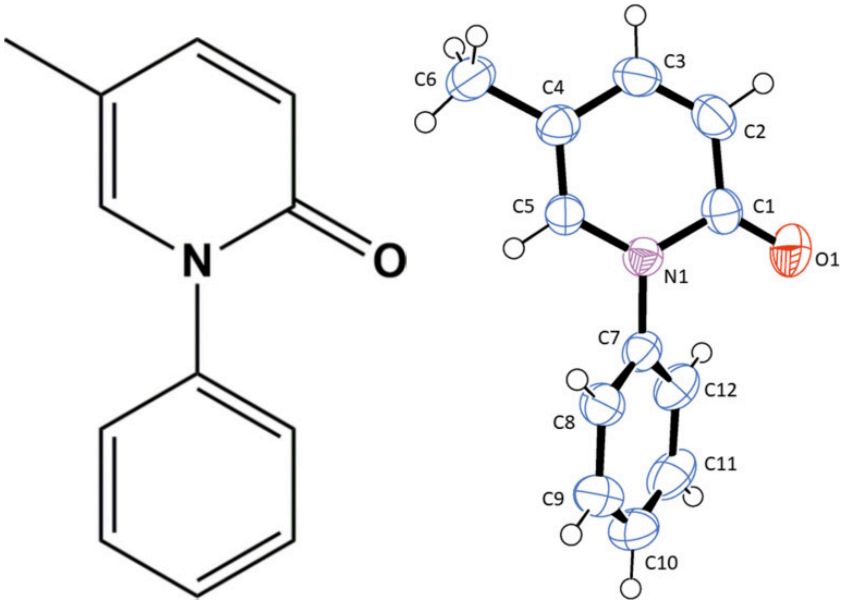

Figure 7: Molecular structure of pirfenidone (Barbero et al.)

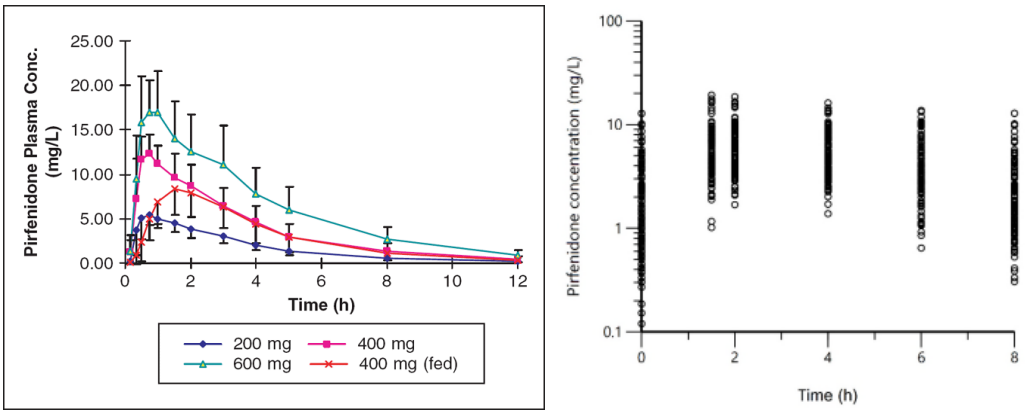

Figure 8: Pirfenidone concentration over time after one-time oral administration of various doses (left)(Shi et al.) and of 400mg (right) (Wang et al.)

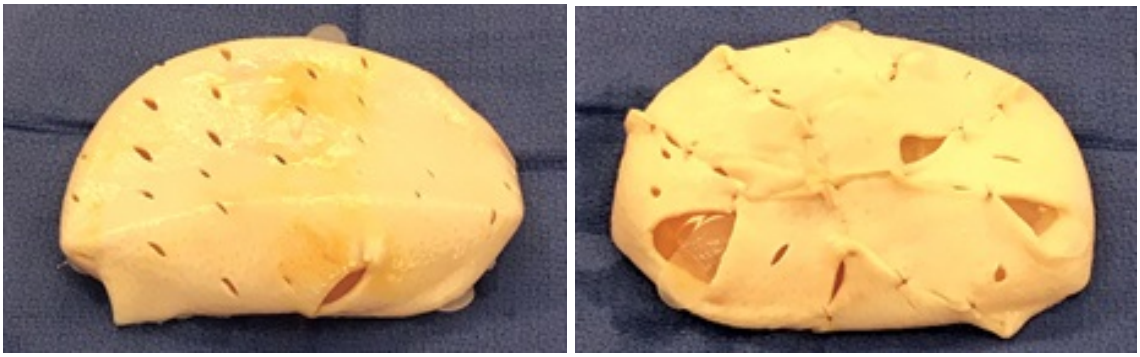

Figure 9: Wanton method for wrapping implant; left image is front, right is back (Sigalove)

Figure 10: Ravioli method for wrapping implant (Sigalove)

Figure 11: Wrapped implant inserted into breast pocket (Nahabedian)

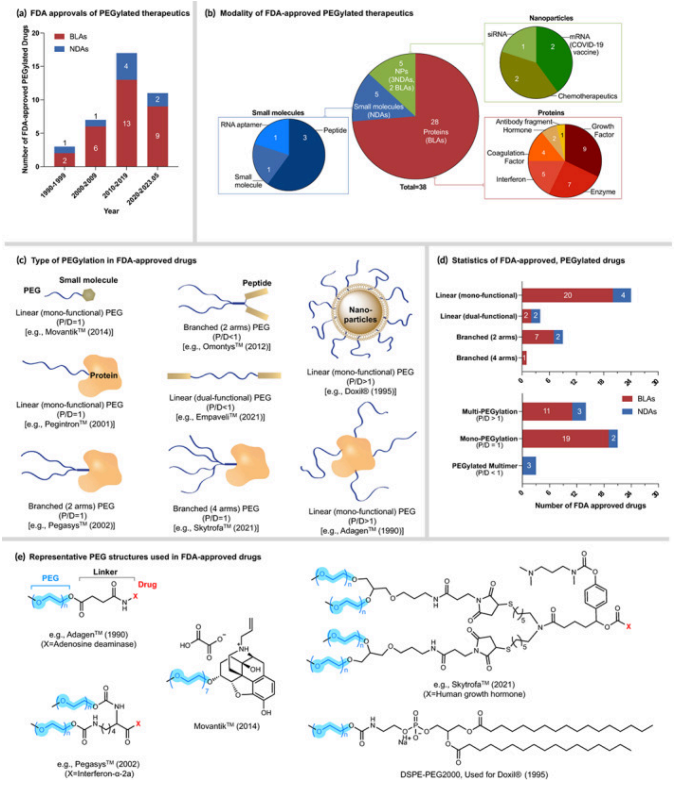

Figure 12: Overview of PEGylation strategies and drugs (Gao et al.)

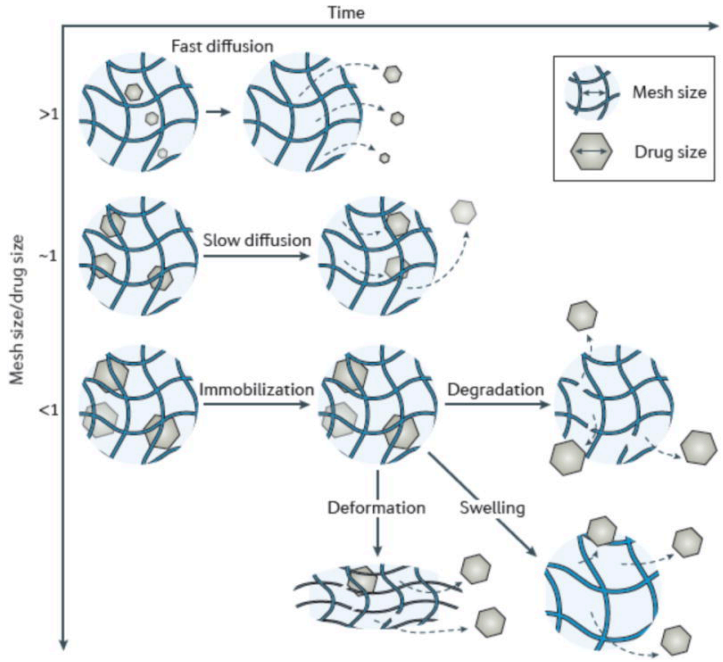

Figure 13: Hydrogel mesh size affects diffusivity rate (Li and Mooney)

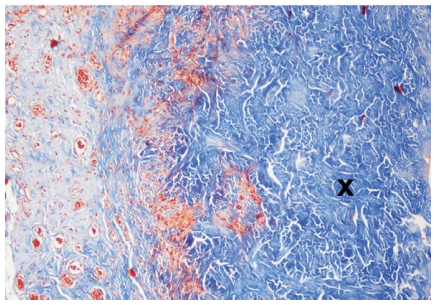

Figure 14: Masson's trichrome stain showing nonlinear collagen architecture (blue) within porcine Strattice ADM (Hester et al.)

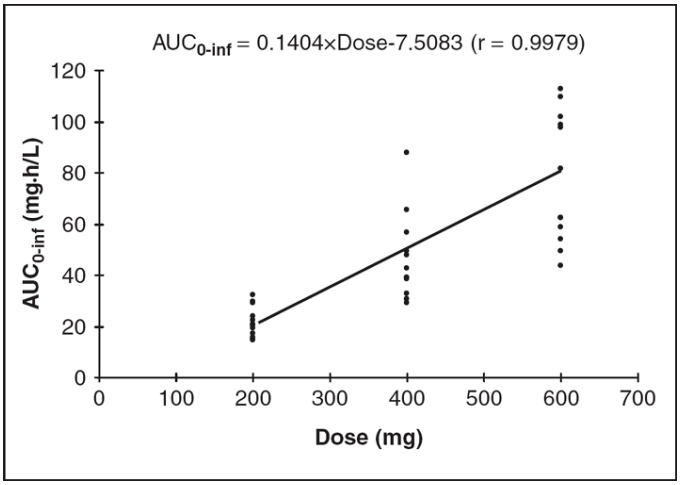

Figure 15: Model for estimating area under the curve pirfenidone concentration by dosage (Shi et al.)

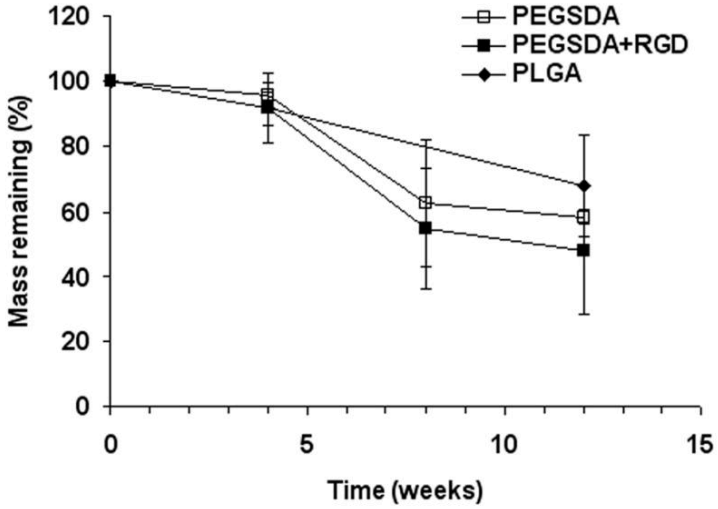

Figure 16: Degradation rate of sebacic acid-based PEG diacrylate implanted subcutaneously in rats as 10mm diameter, 2mm thick disks (Kim et al.)

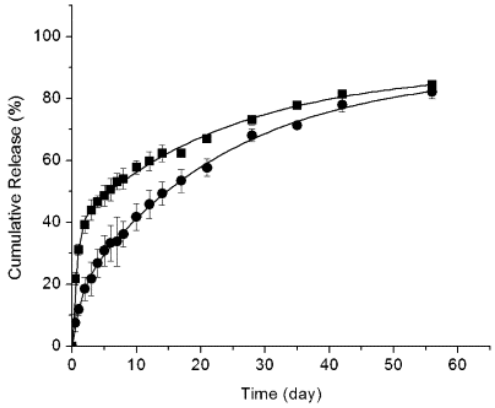

Figure 17: Release of drug from 3.4kDa PEG hydrogel (PBS, pH. 7.4, 37 °C) with ■: 3-sulfanylpropionyl linker, and ●: 4-sulfanylbutyryl linkers. (Schoenmakers et al.)

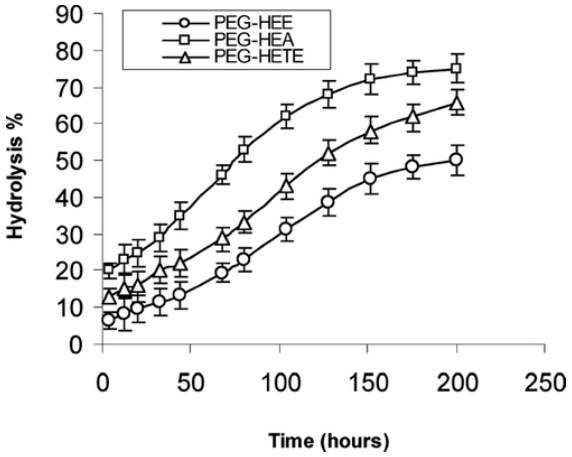

Figure 18: Release of drug from 5kDa PEG (human plasma, pH. 7.4, 37 °C) with hydroxyethyl ester (HEE) linker (Davaran et al.)

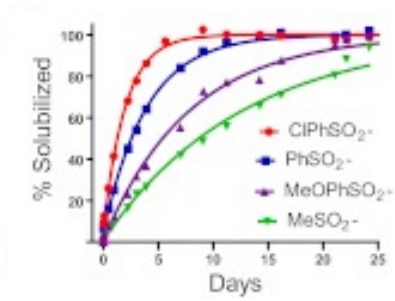

Figure 19: Release rate of drug from 20kDa PEG hydrogel (pH. 7.4, 37 °C) with β-eliminative linkers (Ashley et al.)

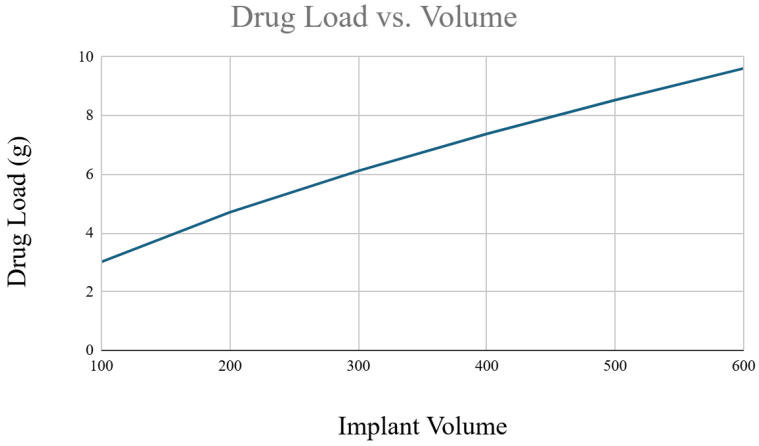

Figure 20: Drug loading capacity of proposed hydrogel

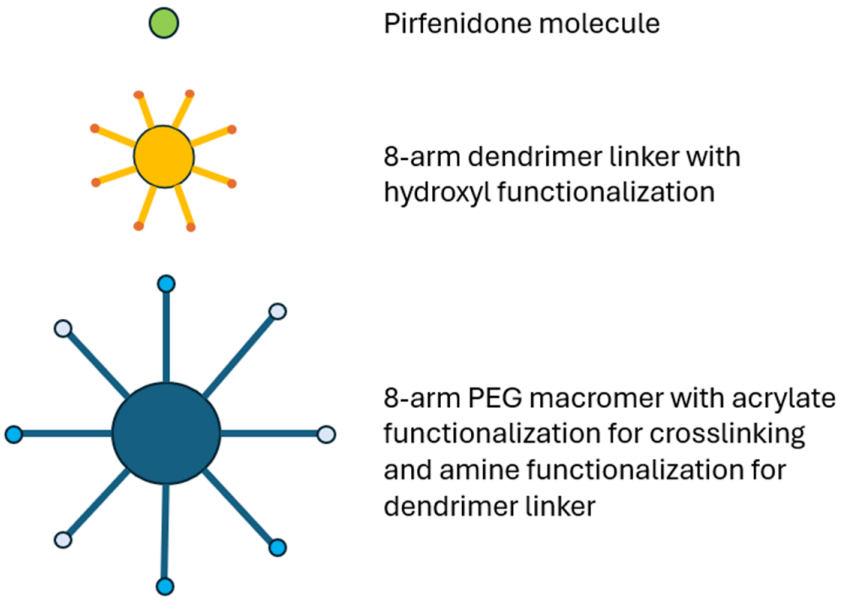

Figure 21: Design components within hydrogel

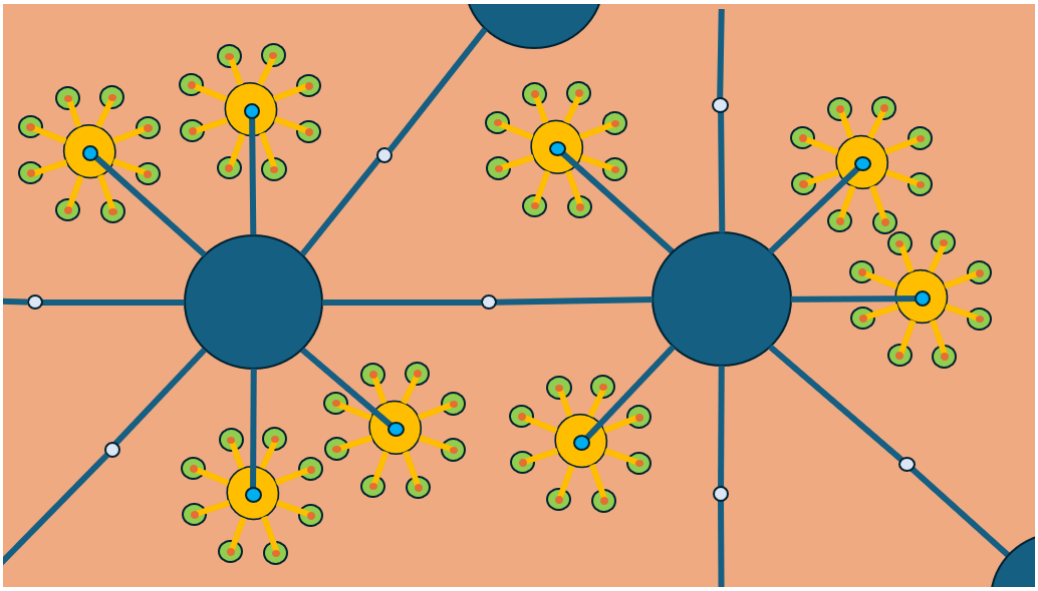

Figure 22: Design components crosslinked as hydrogel within ADM

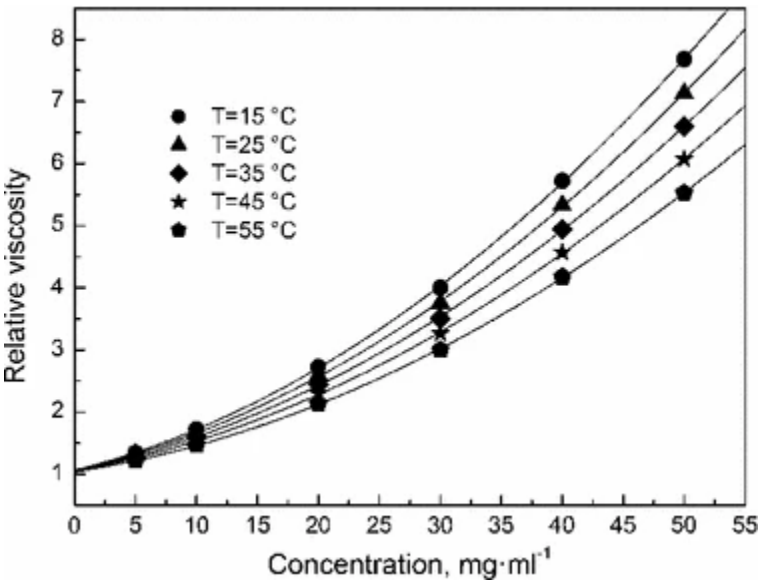

Figure 23: Relative viscosity of 35kDa PEG solution (Tothova et al.)

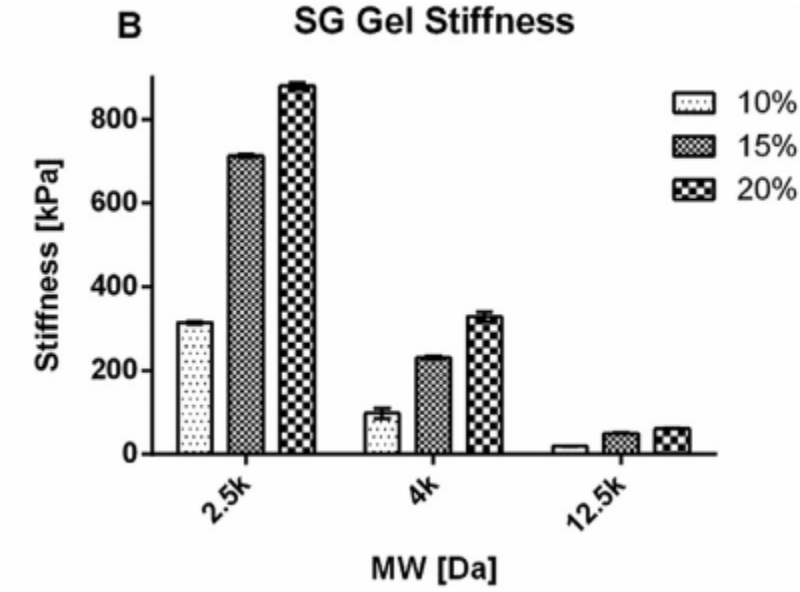

Figure 24: Stiffness of PEG hydrogels at different concentrations and MWs (Lee et al.)

Appendix

Appendix A: Details on EMT Process

Monocytes (which develop in the bone marrow) involved in injury repair are attracted to the site via damage‑associated molecular patterns (DAMPs) (Espinoza et al.; Krzyszczyk et al.). Close to the breast implant surgical site, inflammatory chemokines and cytokines accumulate and promote the expression of cell adhesion molecules that bind the monocytes to the damaged tissue (Krzyszczyk et al.; Alberts et al.). From this bound position, the monocytes differentiate into pro-inflammatory M1 archetype macrophages and anti-inflammatory M2 archetypes to aid in the healing process (Krzyszczyk et al.). M1 archetype macrophages have an ordinary half-life of 20 hours at homeostatic conditions and their numbers in the body fluctuate, but flock to the site of injury and increase in number rapidly during trauma, peaking in concentration around 48 hours after onset (Ogle et al.). These M1 macrophages are responsible for performing phagocytosis to clear away other dead cells and bacteria before releasing chemical signaling molecules to signal the start of M2 macrophage activity (Krzyszczyk et al.).

Entering this second stage of wound healing, M2 macrophages move into the area to begin the process of tissue remodeling through extracellular matrix formation, angiogenesis, re-epithelialization, and wound closure (Krzyszczyk et al.). In this stage, M2 macrophages produce the cytokine TGF-β (activated by the chemical distress signals of the surgery such as hypoxia from cut blood vessels) to aid in cell proliferation and reduce the production of other fibrogenesis mediators, including fibronectin and connective tissue growth factor (Krzyszczyk et al., Zhou et al.). This activated TGF-β binds to transmembrane receptors to transduce the signal via phosphorylation of the SMAD signaling pathway, promoting the expression of EMT genes (Wang et al., Shu et al.).

For the development of a truly capsular contracture preventing implant, it is logical to prevent the development of collagen fiber networks by inhibiting EMT. During EMT, epithelial cells change phenotype and differentiate into myofibroblast cells capable of producing α-smooth muscle actin (α-SMA) and type I collagen (Braga et al.). α-SMA acts as a mechanical reinforcement for the new myofibroblasts that allows the cell to contract, similar to the contractile abilities of smooth muscle fiber (Younesi et al.). Integrated into the produced web of collagen fibers that it has produced and facilitated by the α-SMA, myofibroblasts can contract, resulting in the fibers being pulled and pressure applied around the breast implant (Abu El-Asrar et al.). Current theories suggest that the longer and more interconnected the collagen fibers are, the more likely that CC is to occur (Larsen et al.). Modern treatments, therefore, aim at 1) disrupting the EMT pathway through reduction of signal transduction, 2) reducing the ability of collagen fibers to align and connect, and 3) breaking down existing collagen fiber networks (Hidalgo and Sinno).

To address CC through EMT, early administration of antifibrotic agents is key. In the body, EMT can be determined to take place after the first healing stage after the M1 macrophages have cleaned the area and M2 macrophages have begun to adhere to the wound area, roughly 48 hours after onset (Ogle et al.). In a study of patients who had breast implants for reconstructive purposes, revision surgery to treat capsular contracture occurred at 8.4 years after the initial surgery (Jakob et al.). When compared to the time between initial and revision procedures for aesthetic implant patients in the same study, reconstruction surgery patients required more frequent surgical operations, indicating that early intervention is a necessity for patients receiving a breast implant for reconstructive purposes (Jakob et al.). This proven necessity of earlier intervention for reconstruction patients and the start of EMT 48 hours after surgery suggest that continuously releasing EMT-inhibiting drugs to the site of surgical trauma is a compelling design for high risk patients (Gorgy et al.).

Appendix B: Diffusivity of Pirfenidone

The release profile of therapeutics can be affected by their size relative to the hydrogel's mesh. For large agents, release can accelerate initially as the hydrogel swells and gradually thereafter as the hydrogel begins to degrade. As a small molecule (<1kDa), pirfenidone is significantly smaller than the mesh size of the PEG hydrogel and therefore will diffuse quickly through the hydrogel (Ashley et al.) and into tissue upon cleavage from the PEG hydrogel. Therefore, pirfenidone's rate of diffusion through the PEG hydrogel should not significantly impact the drug's release profile, either by delaying initial release or by accelerating release as the hydrogel degrades. Pirfenidone's diffusion rate can be modeled with the Peppas Equation for the first 60% of release:

$$\frac{M_t}{M_\infty} = 4\left(\frac{Dt}{\pi l^2}\right)^{1/2}$$

Equation 2: Release from thin polymer slab. M_t = total drug released, M_∞ = total drug load, l = thickness, D = diffusion coefficient, t = release time (Ritger and Peppas)

The diffusion coefficient can be approximated from the literature or calculated with the Stokes-Einstein equation.

$$D = \frac{K_b T}{6\pi\eta R_h}$$

Equation 3: Stokes-Einstein equation, where R_h = drug hydrodynamic radius, K_b = Boltzman constant, T = temperature, η = hydrodynamic viscosity of solvent, D = diffusion coefficient (Zhang et al.)

Empirical analysis suggests that the diffusion coefficient for pirfenidone (0.185kDa) is roughly 4×10^{-6} cm^2/s, calculated by linear interpolation between the diffusivities of 5-fluorouracil (0.130kDa) and 1,3-dimethyl-5-fluorouracil (0.199kDa) in 10% 6kDa PEG solution (Mathias et al.). For the same PEG and concentration, the Stokes-Einstein equation gives 3.4×10^{-7} cm^2/s, given T = 298 K, l = 0.002 m, η = 2.545mPa-s (Regupathi et al.), and $R_h = 2.51 \times 10^{-9}$ m (Serrati et al.). For either method, 60% diffusion of the initial drug load completes within 3 hours. This fast diffusion rate confirms that pirfenidone will diffuse quickly through the PEG hydrogel and can enter tissue within hours upon implantation.

Works Cited

A, Kalra, et al. "Mechanical Behaviour of Skin: A Review." *Journal of Material Science & Engineering*, 2016, https://www.hilarispublisher.com/open-access/mechanical-behaviour-of-skin-a-review-2169-0022-1000254.pdf. Accessed 7 May 2025.

Abbasi, Elham, et al. "Dendrimers: synthesis, applications, and properties." *Nanoscale Research Letters*, 2014, https://pmc.ncbi.nlm.nih.gov/articles/PMC4074873/. Accessed 29 April 2025.

Abu El-Asrar, Ahmed, et al. "Macrophage-Myofibroblast Transition Contributes to Myofibroblast Formation in Proliferative Vitreoretinal Disorders." *International Journal of Molecular Sciences, U.S. National Library of Medicine*, 31 Aug. 2023, pmc.ncbi.nlm.nih.gov/articles/PMC10487544/. Accessed 05 May 2025.

Acuner, Burcin, et al. "The Effects of Colchicine-Impregnated Oxidized Regenerated Cellulose on Capsular Contracture." *Surgical Innovation*, 2017, https://journals.sagepub.com/doi/10.1177/1553350617718915?url_ver=Z39.88-2003&rfr_id=ori:rid:crossref.org&rfr_dat=cr_pub%20%200pubmed#bibr13-1553350617718915. Accessed 5 May 2025.

Alberts, Bruce. "Cell-Cell Adhesion." *Molecular Biology of the Cell. 4th Edition., U.S. National Library of Medicine*, 1 Jan. 1970, www.ncbi.nlm.nih.gov/books/NBK26937/. Accessed 05 May 2025.

AlloDerm IFU - Allergan / LifeCell. "Instructions for Use - AlloDerm Regenerative Tissue Matrix." 2020, https://media.allergan.com/products/ADM_ifu_121P0541g_T5-4x6.pdf.

American Society of Plastic Surgeons. "2023 Plastic Surgery Statistics Report." *American Society of Plastic Surgeons*, 2023, https://www.plasticsurgery.org/documents/news/statistics/2023/plastic-surgery-statistics-report-2023.pdf. Accessed 7 April 2025.

Ashley, Gary, et al. "Hydrogel drug delivery system with predictable and tunable drug release and degradation rates." *PNAS*, 2013, https://pmc.ncbi.nlm.nih.gov/articles/PMC3568318/. Accessed 29 April 2025.

Babovic-Vuksanovic, Dusica, et al. "Phase I Trial of Pirfenidone in Children with Neurofibromatosis 1 and Plexiform Neurofibromas." Elsevier, 2007, https://sci-hub.ru/10.1016/j.pediatrneurol.2007.01.009. Accessed 20 April 2025.

Bachour, Yara. "The Aetiopathogenesis of Capsular Contracture: A Systematic Review of the Literature." *Journal of Plastic, Reconstructive & Aesthetic Surgery: JPRAS, U.S. National Library of Medicine*, 5 Dec. 2017, pubmed.ncbi.nlm.nih.gov/29301730/. Accessed 05 May 2025.

Bao, Shixue, et al. "Preparation and evaluation of sustained release pirfenidone-loaded microsphere dry powder inhalation for treatment of idiopathic pulmonary fibrosis." *European Journal of Pharmaceutical Sciences*, 2023, https://www.sciencedirect.com/science/article/pii/S0928098723001392. Accessed 29

April 2025.

Barbero, Mauro, et al. “Crystal structure of pirfenidone (5-methyl-1-phenyl-1H-pyridin-2-one): an active pharmaceutical ingredient (API).” *Acta Crystallographica Section E Crystallographic Communications*, 2019, https://www.sciencedirect.com/org/science/article/pii/S2056989022017042. Accessed 16 April 2025.

Bassetto, Franco, et al. “Complete Implant Wrapping with Porcine-Derived Acellular Dermal Matrix for the Treatment of Capsular Contracture in Breast Reconstruction: A Case–Control Study.” *Aesthetic Plastic Surgery*, 2022, https://pmc.ncbi.nlm.nih.gov/articles/PMC9512749/. Accessed 22 April 2025.

Baumann, Andreas, et al. “Pharmacokinetics, metabolism and distribution of PEGs and PEGylated proteins: quo vadis?” *Drug Discovery Today*, 2014, https://www.sciencedirect.com/science/article/pii/S1359644614002360?via%3Dihub. Accessed 25 April 2025.

Birajdar, Mallinath, et al. “Natural Bio-Based Monomers for Biomedical Applications: A Review.” *Biomaterials Research*, U.S. National Library of Medicine, 1 Apr. 2021, pmc.ncbi.nlm.nih.gov/articles/PMC8015023/#Sec5. Accessed 07 May 2025.

Bohac, Martin, et al. “What happens to an acellular dermal matrix after implantation in the human body? A histological and electron microscopic study.” *European Journal of Histochemistry*, 2018, https://pmc.ncbi.nlm.nih.gov/articles/PMC5806504/. Accessed 25 April 2025.

Bojanic, et al., 2021. “First use of Braxon® acellular dermal matrix for complex revision aesthetic breast surgery—revision augmentation mastopexy.” *Journal of Surgical Case Reports*, 2021, DOI:10.1093/jscr/rjab256.

Braga, Tarcio, et al. “Macrophages during the Fibrotic Process: M2 as Friend and Foe.” *Frontiers*, 24 Nov. 2015, www.frontiersin.org/journals/immunology/articles/10.3389/fimmu.2015.00602/full. Accessed 05 May 2025.

Browning, MB, et al. “Determination of the in vivo degradation mechanism of PEGDA hydrogels.” *Journal of Biomedical Materials Research Part A*, 2014, https://pmc.ncbi.nlm.nih.gov/articles/PMC4112173/. Accessed 23 April 2025.

Capanema, Nádia, et al. “Superabsorbent Crosslinked Carboxymethyl Cellulose-PEG Hydrogels for Potential Wound Dressing Applications.” *International Journal of Biological Macromolecules*, Elsevier, 26 Aug. 2017, www.sciencedirect.com/science/article/pii/S0141813017316756?pes=vor&utm_source=acs&getft_integrator=acs#sec0010. Accessed 07 May 2025.

Carruthers, Christopher, et al. “Histologic Characterization of Acellular Dermal Matrices in a Porcine Model of

Tissue Expander Breast Reconstruction." *PubMed Central*, 2014, https://pmc.ncbi.nlm.nih.gov/articles/PMC4292858. Accessed 17 April 2025.

Chemical Book. "Polyethylene Glycol 6000." *Chemical Book*, 2023, https://www.chemicalbook.com/ProductChemicalPropertiesCB00124577_EN.htm. Accessed 22 April 2025.

Chen, Yuming, et al. "Dexamethasone-loaded injectable silk-polyethylene glycol hydrogel alleviates cisplatin-induced ototoxicity." *International Journal of Nanomedicine*, 2019, https://pmc.ncbi.nlm.nih.gov/articles/PMC6559256/. Accessed 29 April 2025.

Cheng, Angela, et al. "Treatment of Capsular Contracture Using Complete Implant Coverage by Acellular Dermal Matrix." *Plastic and Reconstructive Surgery*, 2013, https://journals.lww.com/plasreconsurg/fulltext/2013/09000/treatment_of_capsular_contracture_using_complete.2.aspx. Accessed 22 April 2025.

Cho, Monique, and Jeffrey Kopp. "Pirfenidone: an anti-fibrotic therapy for progressive kidney disease." *Expert Opinion on Investigational Drugs*, 2010, https://sci-hub.ru/10.1517/13543780903501539. Accessed 16 April 2025.

Costabel, Ulrich, et al. "Pirfenidone in Idiopathic Pulmonary Fibrosis: Expert Panel Discussion on the Management of Drug-Related Adverse Events." *Advanced Therapeutics*, 2014, https://pmc.ncbi.nlm.nih.gov/articles/PMC4003341/. Accessed 21 April 2025.

Craig, Elizabeth, et al. "Outcomes of Acellular Dermal Matrix for Immediate Tissue Expander Reconstruction with Radiotherapy: A Retrospective Cohort Study." *Aesthetic Surgery Journal*, 2019, https://academic.oup.com/asj/article/39/3/279/5002065?login=true. Accessed 17 April 2025.

Dancey, Anne. "Capsular contracture – What are the risk factors? A 14 year series of 1400 consecutive augmentations." *Journal of Plastic, Reconstructive & Aesthetic Surgery*, 2012, https://www.jprasurg.com/article/S1748-6815(11)00536-5/fulltext. Accessed 7 April 2025.

Danko, Dora, et al. "Influencers of Immediate Postmastectomy Reconstruction: A National Cancer Database Analysis." *Aesthetic Surgery Journal*, 2021, https://pmc.ncbi.nlm.nih.gov/articles/PMC9005451/. Accessed 29 April 2025.

Davaran, Soodabeh, et al. "Synthesis and Hydrolytic Behavior of Ibuprofen Prodrugs and their PEGylated Derivatives." *Drug Delivery*, 2005, https://www.tandfonline.com/doi/10.1080/10717540500456007. Accessed 21 April 2025.

Drugs@FDA. "Esbriet Label." *Drugs@FDA*, 2023, https://www.accessdata.fda.gov/drugsatfda_docs/label/2023/208780s007,022535s016lbl.pdf. Accessed 17 April 2025.

Espinoza, Valerie, and Prabhu Emmady. “Histology, Monocytes.” *StatPearls, U.S. National Library of Medicine*, 24 Apr. 2023, www.ncbi.nlm.nih.gov/books/NBK557618/. Accessed 05 May 2025.

Eun Hong, Seung, and Daihun Kang. “Navigating the Pandemic: Shifts in Breast Reconstruction Trends and Surgical Decision-Making in the United States.” *PubMed Central*, 2024, https://pmc.ncbi.nlm.nih.gov/articles/PMC11278449. Accessed 17 April 2025.

FDA, Safety Communication. “Acellular Dermal Matrix (ADM) Products Used in Implant-Based Breast Reconstruction Differ in Complication Rates: FDA Safety Communication.” *FDA Safety Communications*, 2021, https://web.archive.org/web/20220123162747/https://www.fda.gov/medical-devices/safety-communications/acellular-dermal-matrix-adm-products-used-implant-based-breast-reconstruction-differ-complication. Accessed 17 April 2025.

Feng, Xu, et al. “In vivo stiffness measurement of epidermis, dermis, and hypodermis using broadband Rayleigh-wave optical coherence elastography.” *Acta Biomaterialia*, 2022, https://www.sciencedirect.com/science/article/abs/pii/S1742706122002392. Accessed 5 May 2025.

Gancedo, Matias, et al. “Pirfenidone Prevents Capsular Contracture After Mammary Implantation.” *Aesthetic Plastic Surgery*, 2007, https://link.springer.com/article/10.1007/s00266-007-9051-4#ref-CR9. Accessed 7 May 2025.

Gao, Yongsheng, et al. “Covalently Crosslinked Hydrogels via Step-Growth Reactions: Crosslinking Chemistries, Polymers, and Clinical Impact.” *Advanced Materials*, 2025, https://advanced.onlinelibrary.wiley.com/doi/pdf/10.1002/adma.202006362. Accessed 7 May 2025.

Gao, Yongsheng, et al. “PEGylated therapeutics in the clinic.” *National Library of Medicine*, PubMed Central, 2023, https://pmc.ncbi.nlm.nih.gov/articles/PMC10771556/. Accessed 16 April 2025.

Gorgy, Andrew, et al. “Implant-Based Breast Surgery and Capsular Formation: When, How and Why?-A Narrative Review.” *Annals of Translational Medicine*, U.S. National Library of Medicine, 25 Oct. 2023, pmc.ncbi.nlm.nih.gov/articles/PMC10632565/#sec7. Accessed 05 May 2025.

Graziano, Francis, et al. “National Trends in Acellular Dermal Matrix Utilization in Immediate Breast Reconstruction.” *Plastic Reconstructive Surgery*, 2025, https://pmc.ncbi.nlm.nih.gov/articles/PMC11305089/. Accessed 25 April 2025.

Guimier, Eugenie, et al. “Pharmacological Approaches for the Prevention of Breast Implant Capsular Contracture.” *Wound Healing/Plastic Surgery*, Elsevier, 2022, https://www.sciencedirect.com/science/article/pii/S0022480422004589?via%3Dihub. Accessed 7 April 2025.

Hester, Roderick Jr., et al. “Use of Dermal Matrix to Prevent Capsular Contracture in Aesthetic Breast Surgery.”

Plastic and Reconstructive Surgery, American, 2012, https://journals.lww.com/plasreconsurg/fulltext/2012/11002/use_of_dermal_matrix_to_prevent_capsular.20.aspx. Accessed 7 April 2025.

Hidalgo, David, and Sammy Sinno. "Current Trends and Controversies in Breast Augmentation." *Plastic and Reconstructive Surgery*, Journal of the American Society of Plastic Surgeons, 2016, https://journals.lww.com/plasreconsurg/fulltext/2016/04000/current_trends_and_controversies_in_breast.10.aspx. Accessed 7 April 2025.

Huh, Beom, et al. "Elastic net of polyurethane strands for sustained delivery of triamcinolone around silicone implants of various sizes." *Materials Science and Engineering: C*, 2020, https://www.sciencedirect.com/science/article/pii/S0928493119311233?fr=RR-2&ref=pdf_download&rr=9293a872cef48d11. Accessed 7 May 2025.

International Society of Aesthetic Plastic Surgery. "ISAPS Global Survey_2023." *ISAPS*, 2023, https://www.isaps.org/media/rxnfqibn/isaps-global-survey_2023.pdf. Accessed 7 April 2025.

Jakob, Vivian, et al. "Decreasing Time Intervals in Recurring Capsular Contracture? A Single Center Retrospective Study over 6 Years." *Plastic and Reconstructive Surgery Global Open*, U.S. National Library of Medicine, 10 Mar. 2023, pmc.ncbi.nlm.nih.gov/articles/PMC10005826/. Accessed 05 May 2025.

Kim, Jinku, et al. "In Vivo Biodegradation and Biocompatibility of PEG/Sebacic Acid-Based Hydrogels using a Cage Implant System." *Journal of Biomedical Materials Research Part A*, 2011, https://pmc.ncbi.nlm.nih.gov/articles/PMC2928850/. Accessed 23 April 2025.

Krzyszczyk, Paulina, et al. "The Role of Macrophages in Acute and Chronic Wound Healing and Interventions to Promote Pro-Wound Healing Phenotypes." *Frontiers in Physiology, U.S. National Library of Medicine*, 1 May 2018, pmc.ncbi.nlm.nih.gov/articles/PMC5938667/#s3. Accessed 07 May 2025.

Larsen, Andreas, et al. "Histological Analyses of Capsular Contracture and Associated Risk Factors: A Systematic Review." *Aesthetic Plastic Surgery*, U.S. National Library of Medicine, July 2021, pubmed.ncbi.nlm.nih.gov/34312696/. Accessed 05 May 2025.

Lee, Sangdal, et al. "Capsular Contracture Rates in Augmentation Mammaplasty: Comparison of Round vs Anatomical Breast Implants." *Journal of Breast Disease*, 2018, https://www.jbd.or.kr/m/journal/view.php?number=121#:~:text=Capsular%20contracture%20can%20occur%20in,%25%20%5B2%2D6%5D. Accessed 7 May 2025.

Lee, Soah, et al. "Effects of the poly(ethylene glycol) hydrogel crosslinking mechanism on protein release." *Biomaterials Science*, 2017, https://pmc.ncbi.nlm.nih.gov/articles/PMC5127629/#FN1. Accessed 23 April 2025.

Lee, Soah, et al. “The effects of varying poly(ethylene glycol) hydrogel crosslinking density and the crosslinking mechanism on protein accumulation in three-dimensional hydrogels.” *Acta Biomaterialia*, 2014, https://sci-hub.ru/10.1016/j.actbio.2014.05.023. Accessed 7 May 2025.

Li, Jianyu, and David Mooney. “Designing hydrogels for controlled drug delivery.” *Nature Reviews Materials*, 2018, https://pmc.ncbi.nlm.nih.gov/articles/PMC5898614/. Accessed 26 April 2025.

Lin, Zhiqiang, et al. “Novel thermo-sensitive hydrogel system with paclitaxel nanocrystals: High drug-loading, sustained drug release and extended local retention guaranteeing better efficacy and lower toxicity.” *Journal of Controlled Release*, 2014, https://www.sciencedirect.com/science/article/pii/S0168365913008754?via%3Dihub#bb0250. Accessed 23 April 2025.

Luong et al. “Drying and storage effects on poly(ethylene glycol) hydrogel mechanical properties and bioactivityDrying and storage effects on poly(ethylene glycol) hydrogel mechanical properties and bioactivity.” *J Biomed Mater Res A. 2014*, doi: 10.1002/jbm.a.34977.

Macadam, Sheina, and Peter Lennox. “Acellular dermal matrices: Use in reconstructive and aesthetic breast surgery.” *Canadian Journal of Plastic Surgery*, 2012, https://pmc.ncbi.nlm.nih.gov/articles/PMC3383551/. Accessed 25 April 2025.

Mandelbaum, Ava, et al. “National Trends in Immediate Breast Reconstruction: An Analysis of Implant-Based Versus Autologous Reconstruction After Mastectomy.” *Annals of Surgical Oncology*, 2020, https://link.springer.com/article/10.1245/s10434-020-08903-x. Accessed 21 April 2025.

Mathias, Errol, et al. “Properties of small molecular drug loading and diffusion in a fluorinated PEG hydrogel studied by 1H molecular diffusion NMR and 19F spin diffusion NMR.” *Colloid Polym Sci*, 2010, https://pmc.ncbi.nlm.nih.gov/articles/PMC2982959/. Accessed 18 April 2025.

Mowlds, Donald, et al. “Capsular Contracture in Implant-Based Breast Reconstruction Examining the Role of Acellular Dermal Matrix Fenestrations.” *Plastic and Reconstructive Surgery*, 2015, https://journals.lww.com/plasreconsurg/fulltext/2015/10000/capsular_contracture_in_implant_based_breast.1.aspx. Accessed 22 April 2025.

Nahabedian, Maurice. “Current Approaches to Prepectoral Breast Reconstruction.” *Plastic and Reconstructive Surgery*, 2018, https://journals.lww.com/plasreconsurg/fulltext/2018/10000/current_approaches_to_prepectoral_breast.7.aspx. Accessed 17 April 2025.

Namata, Faridah, et al. “Synthesis and Characterization of Amino-Functional Polyester Dendrimers Based On Bis-MPA with Enhanced Hydrolytic Stability and Inherent Antibacterial Properties.” *Biomacromolecules*, 2023, https://pmc.ncbi.nlm.nih.gov/articles/PMC9930107/. Accessed 29 April

2025.

Negishi, Jun, et al. “Application of a Vacuum Pressure Impregnation Technique for Rehydrating Decellularized Tissues.” *Tissue Engineering Part C*, 2014, https://www.liebertpub.com/doi/10.1089/ten.TEC.2013.0654?url_ver=Z39.88-2003&rfr_id=ori:rid:crossref.org&rfr_dat=cr_pub%20%200pubmed. Accessed 25 April 2025.

Oemrawsingh, Arvind, et al. “BREAST-Q Breast-Conserving Therapy Module: Normative Data from a Dutch Sample of 9059 Women.” *Plastic Reconstructive Surgery*, 2022, https://pmc.ncbi.nlm.nih.gov/articles/PMC9586822/. Accessed 24 April 2025.

Ogle, Molly, et al. “Monocytes and Macrophages in Tissue Repair: Implications for Immunoregenerative Biomaterial Design.” *Experimental Biology and Medicine, U.S. National Library of Medicine*, 26 May 2016, pmc.ncbi.nlm.nih.gov/articles/PMC4898192/. Accessed 05 May 2025.

Parcells et al. “Exploration of Robotic Direct to Implant Breast Reconstruction.” *Plast Reconstr Surg Glob Open*, 2020, doi: 10.1097/GOX.0000000000002619.

Patel, Bhupendra, et al. “Breast Implants.” *StatPearls Publishing*, 2022, https://www.ncbi.nlm.nih.gov/books/NBK441998/. Accessed 30 April 2025.

“Pirfenidone.” *National Center for Biotechnology Information. PubChem Compound Database*, U.S. National Library of Medicine, pubchem.ncbi.nlm.nih.gov/compound/Pirfenidone. Accessed 05 May 2025.

Pires, Giovanna, et al. “Comparison of Human, Porcine, and Bovine Acellular Dermal Matrix in Prepectoral Breast Reconstruction.” *Annals of Plastic Surgery*, 2025, https://journals.lww.com/annalsplasticsurgery/abstract/2022/12000/comparison_of_human,_porcine,_and_bovine_acellular.29.aspx. Accessed 22 April 2025.

Pusic, Andrea, et al. “Development of a New Patient-Reported Outcome Measure for Breast Surgery: The BREAST-Q.” *Plastic and Reconstructive Surgery*, 2009, https://journals.lww.com/plasreconsurg/fulltext/2009/08000/development_of_a_new_patient_reported_outcome.1.aspx. Accessed 18 April 2025.

QPortfolio. “Breast-Q.” *QPortfolio*, 2018, https://qportfolio.org/breast-q/breast-cancer/. Accessed 7 April 2025.

Razdan, Shantanu, et al. “National Breast Reconstruction Utilization in the Setting of Post-Mastectomy Radiotherapy.” *Journal of Reconstructive Microsurgery*, 2017, https://pmc.ncbi.nlm.nih.gov/articles/PMC5885287/. Accessed 20 April 2025.

Regupathi, Iyyaswami, et al. “Densities and Viscosities of Polyethylene Glycol 6000 + Triammonium Citrate + Water Systems.” *Journal of Chemical Engineering Data*, 2009, https://sci-hub.ru/10.1021/je9002898. Accessed 21 April 2025.

Ritger, Philip, and Nikolaos Peppas. “A Simple Equation for Description of Solute Release II. Fickian and

Anomalous Release from Swellable Devices." *Journal of Controlled Release*, 1987, https://pdf.sciencedirectassets.com/271103/1-s2.0-S0168365900X01071/1-s2.0-0168365987900356/main.pdf?X-Amz-Security-Token=IQoJb3JpZ2luX2VjEAYaCXVzLWVhc3QtMSJGMEQCIEjCHpQ%2FpIQGK197EsOrCBoN%2FkoP3vstfH%2FiJqR8v06dAiBgBh2YLHAYvKW0Lyxduvna8fyGVR5Ltbk5lCMkDULO. Accessed 19 April 2025.

Roskam, Justin, et al. "The Effects of the COVID-19 Pandemic on Mastectomy Outcomes for Breast Cancer." *Clinical Breast Cancer*, 2023, https://pmc.ncbi.nlm.nih.gov/articles/PMC9951028/. Accessed 7 May 2025.

Safran, Tyler, et al. "Current Concepts in Capsular Contracture: Pathophysiology, Prevention, and Management." *Seminars in Plastic Surgery, U.S. National Library of Medicine*, Aug. 2021, pmc.ncbi.nlm.nih.gov/articles/PMC8432999/. Accessed 05 May 2025.

Schaefer, CJ, et al. "Antifibrotic activities of pirfenidone in animal models." *European Respiratory Review*, 2011, https://pmc.ncbi.nlm.nih.gov/articles/PMC9487788/. Accessed 29 April 2025.

Schoenmakers, Ronald, et al. "The effect of the linker on the hydrolysis rate of drug-linked ester bonds." *Journal of Controlled Release*, 2004, https://www.sciencedirect.com/science/article/pii/S0168365903005716?via%3Dihub. Accessed 21 April 2025.

Sclafani, A P et al. "Evaluation of acellular dermal graft (AlloDerm) sheet for soft tissue augmentation: a 1-year follow-up of clinical observations and histological findings." *Archives of facial plastic surgery*, 2001, https://doi.org/10.1001/archfaci.3.2.101.

Serrati, Simona, et al. "Reproducibility warning: The curious case of polyethylene glycol 6000 and spheroid cell culture." *PLOS One*, 2020, https://pmc.ncbi.nlm.nih.gov/articles/PMC7082040/. Accessed 21 April 2025.

Shi, Shaojun, et al. "Single- and Multiple-Dose Pharmacokinetics of Pirfenidone, an Antifibrotic Agent, in Healthy Chinese Volunteers." *Journal of Clinical Pharmocology*, 2013, https://accp1.onlinelibrary.wiley.com/doi/10.1177/0091270007304104. Accessed 17 April 2025.

Shu, Daisy Y, et al. "EMT and ENDMT: Emerging Roles in Age-Related Macular Degeneration." *International Journal of Molecular Sciences*, U.S. National Library of Medicine, 16 June 2020, pmc.ncbi.nlm.nih.gov/articles/PMC7349630/#sec2-ijms-21-04271. Accessed 05 May 2025.

Sigalove, Steven. "Options in Acellular Dermal Matrix–Device Assembly." *Plastic and Reconstructive Surgery*, 2017, https://journals.lww.com/plasreconsurg/fulltext/2017/12001/Options_in_Acellular_Dermal_Matrix_Device_Assembly.8.aspx. Accessed 17 April 2025.

Smart, Neil. “Supplemental cross-linking in tissue-based surgical implants for abdominal wall repair.” *International Journal of Surgery*, 2012, https://doi.org/10.1016/j.ijsu.2012.07.010.

Spear, Scott, and James Baker. “Classification of Capsular Contracture after Prosthetic Breast Reconstruction.” *Plastic Reconstructive Surgery*, 1995, http://sci-hub.ru/10.1097/00006534-199510000-00018. Accessed 5 April 2025.

Stenstrom, Patrik, et al. “Synthesis and in Vitro Evaluation of Monodisperse Amino-Functional Polyester Dendrimers with Rapid Degradability and Antibacterial Properties.” *Biomacromolecules*, https://pubs.acs.org/doi/full/10.1021/acs.biomac.7b01364. Accessed 8 May 2025.

Tao, Jiang, et al. “Preparation and properties of a new human acellular dermal matrix.” *Chinese Journal of Tissue Engineering Research*, 2016, https://www.cjter.com/fileup/2095-4344/PDF/2016-7-1006.pdf. Accessed 23 April 2025.

Togami, Kohei, et al. “Pharmacokinetic evaluation of tissue distribution of pirfenidone and its metabolites for idiopathic pulmonary fibrosis therapy.” *Biopharmaceutics & Drug Disposition*, 2015, https://onlinelibrary.wiley.com/doi/10.1002/bdd.1932. Accessed 20 April 2025.

Tothova, Jana, et al. “Published: 08 August 2014 Volume 35, pages 2150–2157, (2014) Cite this article Download PDF Access provided by NorthEast Research Libraries (NERL) International Journal of Thermophysics Aims and scope Submit manuscript.” *International Journal of Thermophysics*, 2014, https://link.springer.com/article/10.1007/s10765-014-1707-0. Accessed 7 May 2025.

US FDA. “Summary of Safety and Effectiveness Data: DuraSeal Dural Sealant System.” *Confluent Surgical, Inc.*, 2005, https://www.accessdata.fda.gov/cdrh_docs/pdf4/P040034b.pdf.

Vanitha and Singirikonda. “Development of a Validated Stability Indicating Rp-Hplc Method for the Estimation of Pirfenidone in Bulk Drug and Tablet Dosage Form.” *Journal of Pharmaceutical Research International*, May 2021, journaljpri.com/index.php/JPRI/article/view/2427. Accessed 07 May 2025.

Veras-Castillo, Evelin, et al. “Controlled clinical trial with pirfenidone in the treatment of breast capsular contracture: association of TGF-β polymorphisms.” *Annals of Plastic Surgery*, 2013, https://sci-hub.ru/10.1097/sap.0b013e31822284f4. Accessed 28 April 2025.

Vigata, Margaux, et al. “Hydrogels as Drug Delivery Systems: A Review of Current Characterization and Evaluation Techniques.” *PubMed Central*, 2020, https://pmc.ncbi.nlm.nih.gov/articles/PMC7762425/. Accessed 19 April 2025.

Vinsensia, Maria, et al. “Incidence and Risk Assessment of Capsular Contracture in Breast Cancer Patients following Post-Mastectomy Radiotherapy and Implant-Based Reconstruction.” *Incidence and Risk Assessment of Capsular Contracture in Breast Cancer Patients following Post-Mastectomy Radiotherapy and Implant-Based Reconstruction*, 2024,

https://pmc.ncbi.nlm.nih.gov/articles/PMC10813520/. Accessed 7 April 2025.

Wang, Peile, et al. “Multicenter Population Pharmacokinetics and Exposure–Efficacy Analysis of Pirfenidone in Patients with Idiopathic Pulmonary Fibrosis.” *Clinical Pharmacokinetics*, 2023, https://link.springer.com/article/10.1007/s40262-023-01250-6. Accessed 26 April 2025.

Wang, Qi, et al. “SMAD Proteins in TGF-β Signalling Pathway in Cancer: Regulatory Mechanisms and Clinical Applications.” *Diagnostics (Basel), U.S. National Library of Medicine*, 26 Aug. 2023, pmc.ncbi.nlm.nih.gov/articles/PMC10487229/. Accessed 05 May 2025.

Webster, Rob, et al. “PEGylated Proteins: Evaluation of Their Safety in the Absence of Definitive Metabolism Studies.” *The American Society for Pharmacology and Experimental Therapeutics*, 2006, https://sci-hub.ru/10.1124/dmd.106.012419. Accessed 23 April 2025.

Younesi, Fereshteh, et al. “Fibroblast and Myofibroblast Activation in Normal Tissue Repair and Fibrosis.” *Nature News, Nature Publishing Group*, 8 Apr. 2024, www.nature.com/articles/s41580-024-00716-0. Accessed 05 May 2025.

Zammit, Dino, et al. “Meshed acellular dermal matrix: technique and application in implant based breast reconstruction.” *Plastic and Aesthetic Research*, 2016, https://www.oaepublish.com/articles/2347-9264.2015.128. Accessed 22 April 2025.

Zang, Chunbao, et al. “Hydrogel-based platforms for site-specific doxorubicin release in cancer therapy.” *Journal of Translational Medicine*, 2024, https://pmc.ncbi.nlm.nih.gov/articles/PMC11440768/. Accessed 29 April 2025.

Zhang, Ruquan, et al. “Rheological and controlled release properties of hydrogels based on mushroom hyperbranched polysaccharide and xanthan gum.” *International Journal of Biological Macromolecules*, 2018, https://sci-hub.ru/10.1016/j.ijbiomac.2018.09.008. Accessed 19 April 2025.

Zhang, Yongwei, et al. “Water absorption by decellularized dermis.” *Heliyon*, 2018, https://pmc.ncbi.nlm.nih.gov/articles/PMC5968173/. Accessed 23 April 2025.

Zhou, Chaoming, et al. “Anti-fibrotic action of pirfenidone in Dupuytren’s disease-derived fibroblasts.” *BMC Musculoskeletal Disorders*, 2016, https://pmc.ncbi.nlm.nih.gov/articles/PMC5106805/. Accessed 20 April 2025.